47TH TURBOMACHINERY & 34TH PUMP SYMPOSIA
HOUSTON, TEXAS | SEPTEMBER 17-20, 2018
GEORGE R. BROWN CONVENTION CENTER

MULTIDISCIPLINARY APPROACH TO FAILURE ANALYSIS OF TURBOMACHINERY COMPONENTS

Kirill Grebinnyk, P.E.
Lead Engineer
Sulzer
La Porte, TX, USA

Vamadevan Gowreesan, PhD
Sr. Materials and Welding Engineer
Sulzer
La Porte, TX, USA

Ricardo Guerrero, P.E.
Mechanical Design Engineer
Sulzer
La Porte, TX, USA

Kirill Grebinnyk is a Lead Engineer at Sulzer Rotating Equipment Services (RES) division, working in the Service Center located in La Porte, TX. With more than 10 years of experience in fluid dynamics, finite-element methods and design of turbomachinery, he is in charge of Sulzer's program of aerodynamic rerates and upgrades of turbomachinery. Kirill's area of professional expertise includes failure analysis, structural and modal analysis and testing of the rotating equipment. He is a licensed Professional Engineer in Texas and holds a Masters in Mechanical Engineering.

Dr. Gowreesan is a Senior Materials and Welding Engineer at Sulzer Rotating Equipment Services (RES) division, working in the Service Center located in La Porte, TX. He has been working in the turbomachinery field for more than ten years. His experience includes metallurgical root cause failure analysis, selection and qualification of materials for different components of turbomachines, development of welding procedures and troubleshooting materials and welding related issues in the repair of steam and gas turbines, centrifugal compressors, hot gas expanders. He has conducted more than 50 metallurgical root cause failure analysis of different turbomachines components.

Ricardo Guerrero is a Mechanical Design Engineer at Sulzer Rotating Equipment Services (RES) division, working in the Service Center located in La Porte, TX. He has been with Sulzer for five years and is primarily responsible for stress analysis and fracture mechanics. Ricardo is a licensed Professional Engineer in Texas and holds a Masters in Mechanical Engineering Design.

ABSTRACT

This tutorial is intended to provide insight into the failure analysis approach taken by the authors for various turbomachinery equipment, such as steam turbines, axial and centrifugal compressors and hot gas expanders. Successful failure analysis is crucial for making the right decisions to mitigate similar types of failure in the future. Whether a failure was caused by an inherent design flaw, improper operating practices or any other combination of factors, it is important to have a comprehensive understanding of the mechanisms that led to failure to be able to correctly address them.

INTRODUCTION

Modern turbomachinery can be regarded as sophisticated equipment due to the manufacturing and assembly tolerances involved, the complex alloys used for its components, the demanding operating conditions and aggressive environments. Additionally, the end-users of turbomachines are expecting the highest degree of reliability, availability and long service intervals. The potential failure modes are becoming more unpredictable and complex as turbomachinery OEMs are striving to meet their clients' needs and making the equipment even more sophisticated.

A large number of legacy turbomachines are installed and operating at plants across different industries. However, the plant's demands, process conditions and operating procedures are changing, and sometimes quite significantly. For various reasons, some of the changes in the processes and regimes are not necessarily recognized and documented by plant personnel. Indirectly, this leads to operating the equipment outside the design envelope. Along with some of the components reaching their end of useful life, this may lead to completely unexpected failures, at first glance. Only after a detailed investigation and design review can the underlying causes for such failures can be discovered and addressed.

In the first section, this tutorial will summarize the steps for successful failure analysis and the most common failure mechanisms in such equipment as centrifugal compressors, steam turbines and hot gas expanders. In the second section, the tutorial the case studies will be presented to describe the techniques employed across multiple disciplines to understand the underlying causes of failures and corrective actions necessary to address them.

GENERAL APPROACH TO FAILURE ANALYSIS

To succeed in the failure investigation, it is crucial to examine each case from a few distinctly different aspects and understand how they interact and affect each other to result in a failure. General consistency in the approach and steps taken is highly important for a success analysis. Over the years, the authors have established a framework within which the following distinct steps can be identified:

- General details
- Materials (metallurgical) aspect
- Design aspect
- Operational aspect
- Summary of findings

An in-depth understanding of each step is essential for an individual, or a team, performing a failure analysis to be successful. Visual representation of this framework is presented in Figure 1. The steps are discussed in detail below.

General Details

A good way to start a failure analysis would be to look at the big picture, understand what equipment and components have failed and visually assess its conditions and damages. The first steps would be to collect and protect the physical evidence: attempt to find and recover remaining failed components, visually examine the fracture surfaces, document the appearance and preserve them until the equipment can be disassembled and a failed part can be removed for fractography.

At this initial step, it is also worth collecting and confirming some general information regarding the particular equipment and entire machinery train it operates within. The critical information includes the nameplate performance data, nature of service and load conditions, history of maintenance and repairs and any unusual service conditions or events preceding the failure. A lot more information in each respective area would be required to get to an appropriate level of detail during the failure analysis. However, knowing the significant facts before taking any further steps will enable the engineer involved with the investigation (or a team of experts) to make more informed decisions about the tests required and analysis methods throughout the process.

Failure Analysis Framework

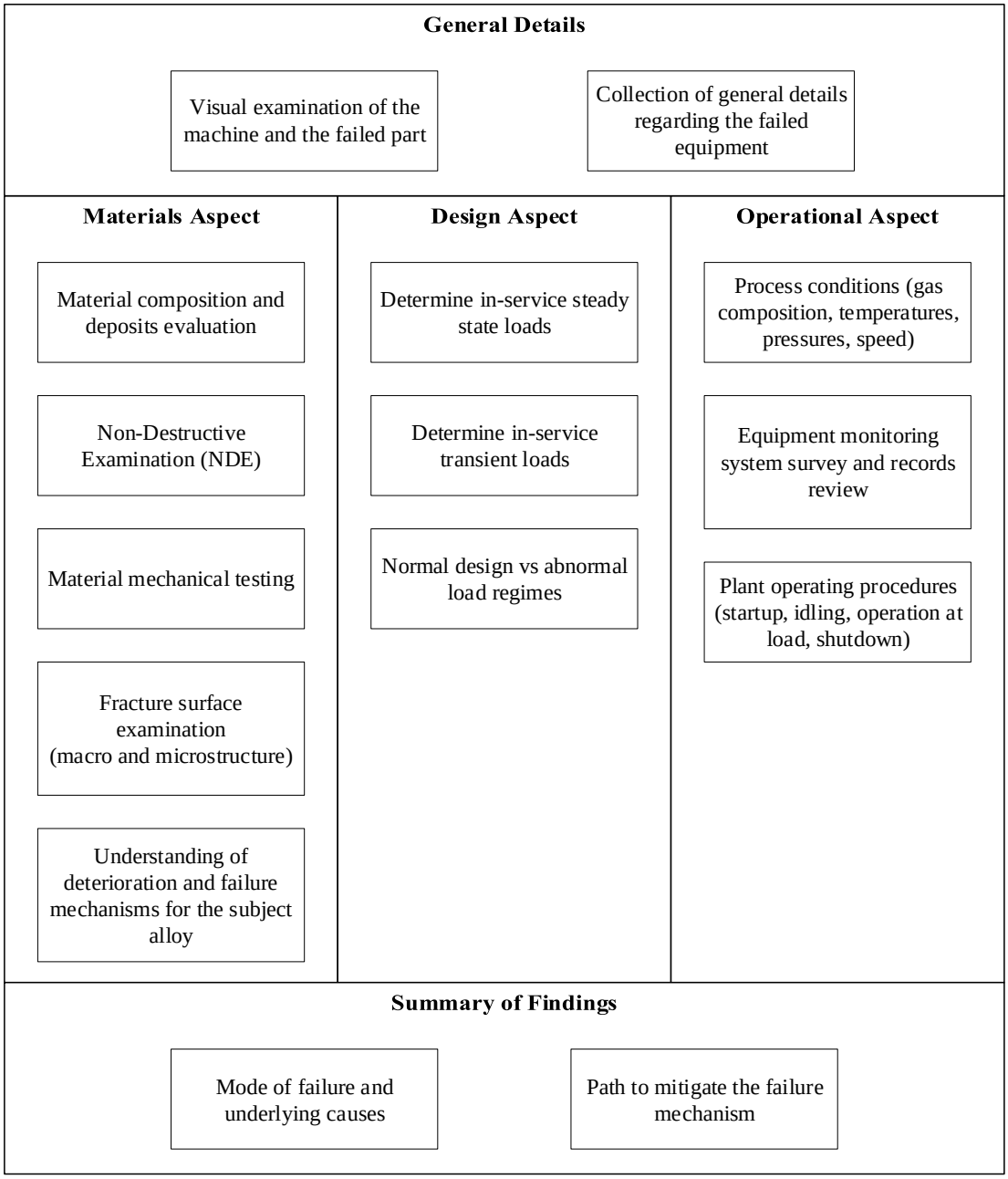

Figure 1: Failure Analysis Framework

Materials Aspect

Metallurgical root cause failure analysis helps identify information related to a failure. Analysis of the fracture surface (or fractography) is the main component of a metallurgical failure analysis. Fractrography involves pattern matching of features found on the fracture surface to features relevant to different modes of failures.

The evaluation starts with a simple visual inspection of the fracture surface or its direct replica. A direct replica of the fracture surface is obtained and used for the analysis in cases where a portion of the fracture surface cannot be cut from the part for the microscopic analysis. The evaluation will then progress into an analysis with stereo microscope, scanning electron microscope (SEM) and transmission electron microscope (TEM). The analysis looks for the primary mode (mechanism) of failure, the failure initiation site, material defects, manufacturing defects etc. Each failure mode has its own telltale signs and appearance of the fracture surface. Common failure modes and a visual representation of each are included below. Also, a short history of fractrography including a discussion of most common fracture surface features can be found in Lynch and Moutsos (2006).

The following main steps outline the metallurgical part of the failure investigation.

Material positive identification and chemical analysis of the base metal and foreign deposits

Understanding of the alloy type and composition of the failed part is the first step in the material assessment. Correctly identifying an alloy allows the engineer to make an educated guess on its mechanical properties, determine the chemical compatibility between the alloy and service fluid, and define the scope and limitation of the analysis (such as non-destructive examination). Any inclusions or foreign deposits should be carefully studied. Very often the amount of foreign deposits, their nature and specific location are quite helpful in understanding the timeline of the fracture's initiation and propagation. Areas for testing and specimen collections have to be carefully selected, and it is highly preferable to perform testing before blast media, cooling fluid or any other external agents make contact with the base material.

Non-Destructive Examination (NDE) of the failed component

Although most attention is typically paid to the failed component in the assembly (or failed area of an individual component), it is important to inspect the whole assembly for damages and incipient indications. Presence of indirect evidence might be as important as direct evidence. Some of the indications discovered may have a similar nature to the ones that led to a failure, but be in the propagation phase. Therefore, opening and studying them will provide a comparison to the main fracture surface, where the actual failure occurred.

Macroscopic and microscopic examination of the fracture surface and any other remaining evidence

To understand the failure mechanism, it is critical to understand where and how the fracture initiated, how it propagated, for how long it propagated and where the final failure occurred. Preservation of a fracture surface by covering it in a protective compound should be done immediately after thorough dimensional and photographic evidence are collected. Microscopic examination can also provide evidence with regards to the presence, or absence, of material deterioration mechanisms. The following deterioration mechanisms are the most common in turbomachinery components: embrittlement, grain coarsening and dislocation, material impurities and their location within the grains or boundaries.

Hardness and mechanical testing

Hardness testing is the easiest way to estimate the mechanical properties of a material. A best practice is to test multiple locations on a part. The areas around the failure zone should be tested even more thoroughly and compared to the values obtained from the unaffected areas of the part. For smaller areas, microhardness traverse can provide useful information as well. However, the hardness readings within the expected range may not necessarily indicate good condition of the material. In some cases, a few competing deterioration mechanisms may affect the parts with some of them causing hardening, while the others are resulting in softening. Also, not having the exact hardness specifications for a virgin material makes things more complicated for the investigator.

Mechanical testing (tensile, impact, toughness) can be performed if deemed necessary and if sufficient material is available to make specimens. Before extracting the test specimens, it is advised to confirm that they are going to be representative of the failed location by comparing hardness and microstructure. If a failure mechanism is suspected to be related to high temperature deterioration, a stress-rupture and creep testing may provide an additional information about the material condition.

Design Aspect

A thorough understanding of the equipment design, methods of parts fabrication and assembly, as well as types and sources of loading occurring in the studied equipment is extremely important for a successful investigation. Without this, it would be impossible to address one of the major concerns of all parties involved in the investigation – whether the failure is caused by a pre-existing design flaw, deterioration of material or if the original design was sound, but the equipment had been operated outside of the intended design envelope. The following aspects of a failed part design need to be studied and understood:

- Determine sources of loading – rotational force, thermal gradients, gas loading forces.
- Determine the static (steady state) and cyclic (alternating) loads acting on equipment and its components.
- Is the type and amount of load typical for the unit or was there an abnormal event involved.

Engineering calculations or simulations (finite-element analysis (FEA), computational fluid dynamics (CFD)) are usually performed to determine the stresses under design and off-design loading conditions. Some of the trade-offs that an engineer performing such investigation faces is whether the engineering simulation needs to include all possible assembly parts, their unique geometry details and all loading conditions. Evaluating the model with all possible details and multiple load conditions may be time consuming. In contrast, some of the loads and geometrical features can be considered as insignificant and dismissed to reduce the simulation time and complexity. It is difficult to provide universal guidance on how to draw a boundary between including too many details and making a simulation unnecessarily complicated versus intentionally oversimplifying the model. For example, important results can be missed if some loads are neglected, and the engineer will be unable to draw the right conclusions. Engineering experience of a person or a team members along with sound engineering judgements can typically provide a good starting point for the numerical analysis.

Based on evidence obtained from a metallurgical evaluation, preliminary conclusions can be made and failure theories can be narrowed, with some hypothesis being excluded as unfeasible. Knowing these findings helps to improve judgement about the loads that can be ignored during simulation and provides an additional emphasis for accurate evaluation of the failed design.

Operational Aspect

Evaluation of the operational aspect of the failure is often overlooked by engineers performing failure analysis, but it is as important as the other abovementioned aspects. Without knowing the specifics regarding operation of the equipment and its design boundaries, it is nearly impossible to draw the right conclusions about whether the failure observed is a pre-existing design flaw or the result of operation outside of its original design boundaries (regardless whether it was intentional or not).

The operational aspect becomes even more critical when it comes to failures of legacy equipment. For such equipment, the OEM manuals might not be available, initial design conditions and considerations are not clearly known and some of the modifications that have been done to the equipment in the past were not properly documented. It is not unusual to see some of the refineries and chemical plants change owner companies as well as engineering and operational personnel. At the same time, the level of recordkeeping varies significantly across the industry from exceptional at some plants to virtually non-existing at others. In addition, it is highly preferable to have a clear picture of all the initial design parameters and their modifications not only for the equipment, which is a primary subject of a failure analysis, but also for the rest of the train.

These days, most of the plants have their critical rotating equipment almost fully instrumented and continuously monitored when it comes to such critical indicators such as radial and axial vibrations and displacements, bearing temperature, lube oil parameters and process conditions (temperatures, pressures, flows). However, having the instrumentation merely installed is not sufficient, it is important to have a high degree of confidence in the accuracy of its calibration and consistency of the readings provided. Sometimes during a failure investigation there might be serious and well-supported doubts about instrumentation accuracy and integrity of its readings. In these cases even a single faulty or ill-calibrated transducer may set a precedent to invalidate an entire layer of data, which would be important for a proper failure investigation.

The following information about the equipment and the train, if available, can provide a useful insight into the operational aspect of a failure:

- Verbal accounts of an incident occurred
- Service history - amount of time the equipment and parts have been in service since initial commissioning and timeline of the outages, operating hours and starts)
- Monitoring and controls system data (operating speed, vibration, process conditions)
- Changes in the train configuration, plant operating procedure and process conditions since the equipment has been originally installed

Summary of Findings

Drawing conclusions about the mode of failure and underlying causes of it based on the findings is the most challenging part of the process. For this step, it is difficult to offer one solution that would fit all potential cases. Inevitably, even engineers with significant experience are not going to correctly identify the problem unless at least some of the minimum required evidence is available. However, from the authors' experience, following the framework established above improves the chances of a successful outcome.

Another problem that almost everyone directly involved in failure analysis is facing is how much evidence is sufficient for providing accurate conclusions. In this matter, some engineers and companies may end up on different ends of the spectrum: while some think that it is sufficient to collect and examine the bare minimum of data and jump to conclusions, others tend to double-check and triple-confirm every piece of information which may require a significant amount of time and resources to obtain.

Is there a golden mean? And if there is, does it have to be the same every time, or how would the investigator correctly define it for each and every case? The answer to this can be boiled down to such considerations as criticality of the equipment for the process, monetary losses caused by the failure (including direct damage and indirect losses, such as lost production or other business opportunities), and last, but the most important, impacts of such failure on safety of the personnel in the workplace. From the commercial standpoint it is difficult to justify spending significant money and resources to investigate a failure in the equipment that can be easily replaced or upgraded because its impacts on the plant operations are minimal. In contrast, for highly critical equipment, which recurring failure may have catastrophic outcomes for the plant production or have an imminent impact on personnel safety, significant resources have to be dedicated for a failure investigation and prevention.

FAILURE MODES

Failure can occur in a single mode or in a combination of different modes. The following are the most common modes of failures seen in turbomachines:

- Ductile Overload Failure
- Brittle Failure
- Fatigue Failure
- Corrosion Related Failure
- Stress Corrosion Cracking
- Embritlement Related Failure
- Creep Failure

This section describes specifics of each failure mode such as some general design and operating considerations and typical findings from visual inspections, material properties and microscopic analysis.

Ductile Overload Failure

This mode of failure corresponds to a failure with appreciable amount of plastic deformation prior to failure. This means that the stress at the failure location is greater than the yield strength of the material. Typical causes of component failure in ductile overload are:

- Operation outside of the normal conditions (rotational speed, temperature)
- Insufficient material strength

Operating outside of the design envelope for the equipment, for example overspeed above the maximum operating speed or process temperature increase above the design level, may lead to an overload failure. It is important to remember that for most materials the strength is decreasing with increase in temperature, therefore temperature excursions beyond the design ranges even for short time may lead to a failure in the equipment.

The causes of insufficient material strength can be due to improper selection of the material for the known stress level (or incorrect stress level assessment) or incorrect material manufacturing or part fabrication process (heat treatment, welding) resulting in reduced mechanical properties or elevated residual stresses.

At the same time, turbomachinery components are often times designed with some amount of localized yielding and plastic deformation. For example, steam turbine blades are typically designed to have localized stresses close to yield strength of the material in the root section fillets. An example of such stress concentration predicted by a linear-elastic FEA is shown in Figure 2.

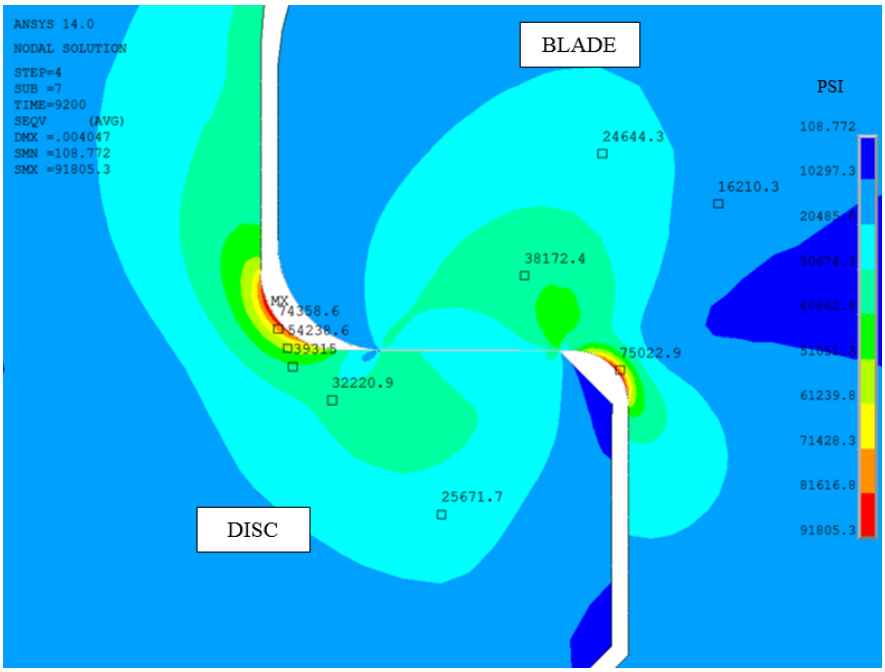

Figure 2: Stress Concentration in Turbine Blade and Disc Fillets Predicted by FEA

It is important to note that even though some of the linear-elastic structural FEA results may display localized stresses close or

even above yield strength of material, their presence does not necessarily indicative of an improper design with ductile overload in the part. If the elevated stress regions are highly localized, then strain hardening and plastic deformations will, in most cases, result in redistributing the stress concentrators.

This approach can only be applied for the materials with sufficient plasticity past the point where material reaches its yield strength. Yield strength to ultimate tensile strength ratio equal to 0.85 or less can be used as a criterion of sufficiently ductile material, for which it is permissible to have localized plastic deformations. Non-linear (elastic-plastic) analysis can be done for the complex cases. For such non-linear analyses, the investigator should use the stress-strain curve obtained from tensile testing a specimen from the actual part, preferably at a temperature close to the operating temperature.

In addition, the material should have considerable ductility for this failure mechanism to occur. SEM evaluation of the fracture surface would show dimples. A sample fractrograph showing a ductile failure with dimples is shown in Figure 3.

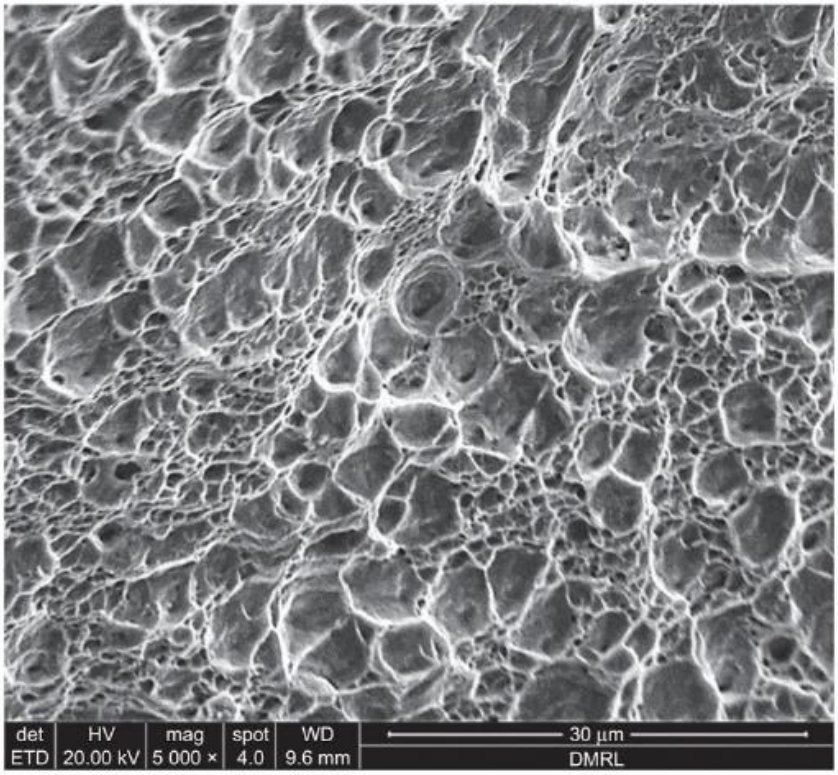

Figure 3: Fractrography Showing Dimples (Balan, (2018))

Brittle Failure

Brittle failure occurs rapidly without any noticeable macroscopic plastic deformation. Depending on the nature of the brittle failure, the fracture surface may exhibit a chevron pattern or herringbone pattern. This pattern shows the direction of crack propagation and also points to the crack orientation. This pattern is particularly pronounced in plate-like parts such as impellers and discs. A sample fracture surface with chevron marks is shown in Figure 4. The arrows point to some of the chevron marks on the fracture surface. The pattern of the chevron marks shows that the crack initiated at the right side and propagated to the left. The brittle fracture surface may or may not have a visible "river" pattern on the fracture. The "river" pattern shows information of the crack initiation location and propagation direction.

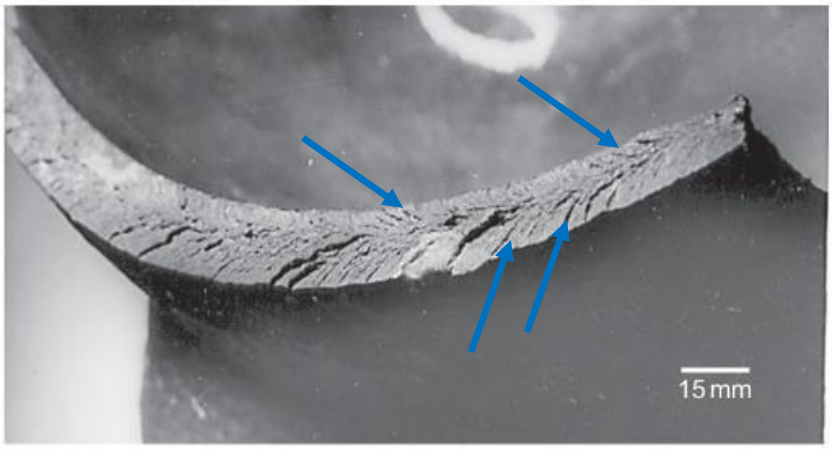

Figure 4: A Sample Fracture Surface with Chevron Marks (Lynch and Moutsos (2006))

Brittle fracture may show cleavage features when examined with a scanning electron microscope. Figure 5 shows a sample SEM image of a cast part that failed in a brittle manner. The arrows in the figure point to some of the cleavage facets on the fracture surface.

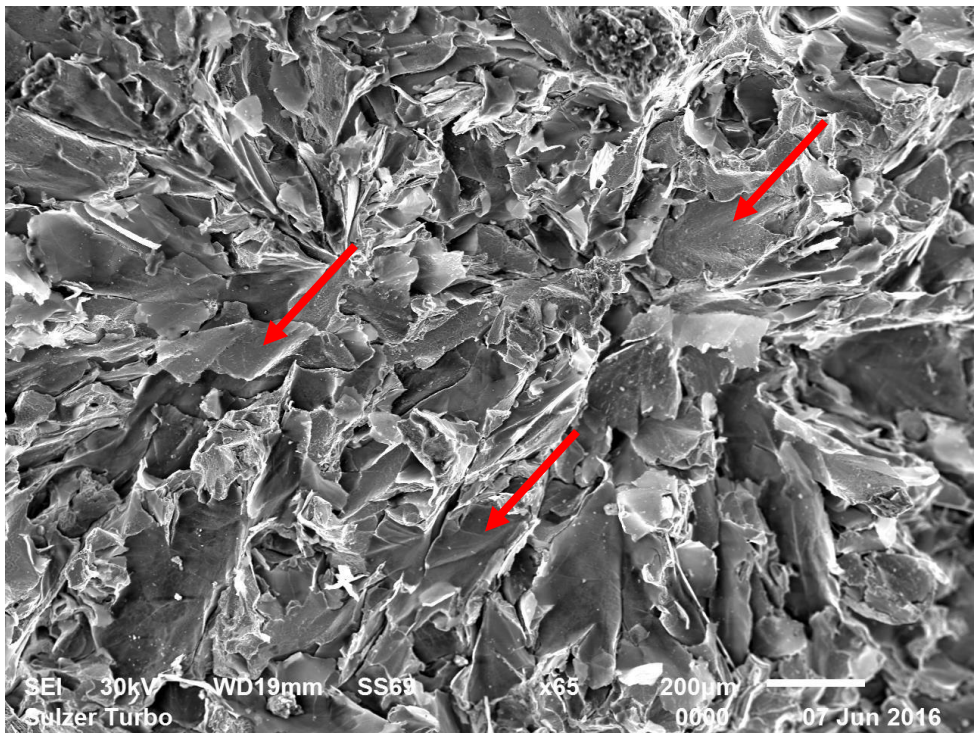

Figure 5: SEM image showing cleavage fracture in a cast part used in a steam turbine.

Fatigue Failure

It can be said that fatigue is one of the most common failure mechanisms in turbomachinery parts. Fatigue failure occurs when cyclic (alternating) stress acts on a part. When the alternating stresses are high enough, localized damage to the material occurs with each load cycle at a microscopical level. The crack propagates with continued cyclic or fluctuating stresses.

Two modes of fatigue are typically recognized and distinguished: high-cycle and low-cycle fatigue. High-cycle fatigue (HCF) is characterized by low amplitude of stress applied to component at high frequency. The most common cause of HCF in turbomachinery are vane passing frequencies – periodic interactions between the stationary vanes and rotating blades. Vane passing frequencies have relatively small stress amplitudes, but the load alternates multiple times during each revolution of the rotor. Low-cycle fatigue (LCF) is defined as high stress amplitude applied with a relatively low frequency. LCF can occur due to thermo-mechanical loads when equipment is subjected to transient operating conditions (startup, shutdown, trip, restart). The number of cycles to failure for LCF is defined as less than 10,000. The failure mechanism is considered to be HCF if the fatigue failure occurs after more than 10,000 cycles.

The most common tools for evaluating fatigue life and understanding fatigue failures of the components are material's S-N curves and fatigue-life diagrams, such as Goodman or Soderber diagrams. The S-N curve for a material provides an estimated number of load cycles it can withstand under a certain alternating stress before fatigue failure. The stress under which the material will not fail before it experienced 10^7 cycles is defined as the fatigue strength of a material (often referred to as fatigue limit or endurance limit). A generic example of an S-N curve for steel is shown in Figure 6.

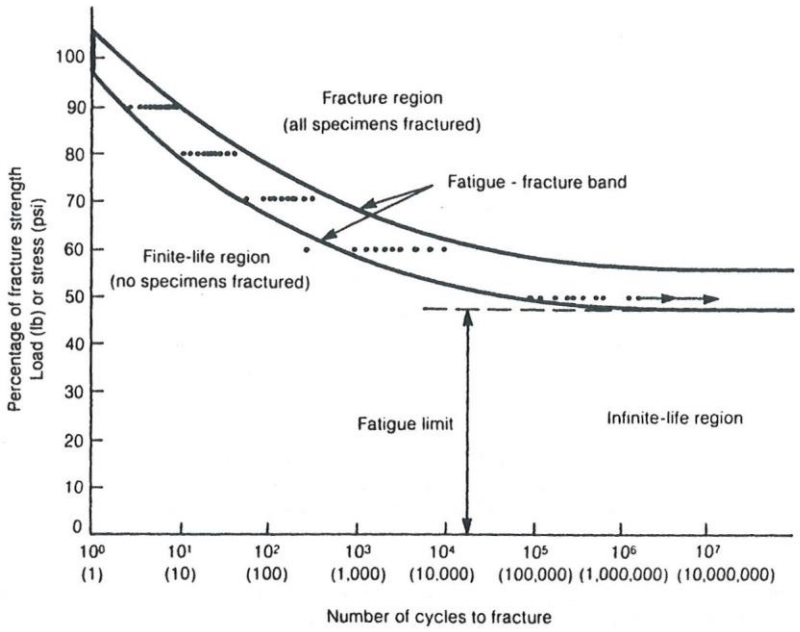

Figure 6: Generic S-N Curve Example for Steel (Boyer (1986))

If mean and alternating stresses are known, Goodman or Soderberg diagrams can be used to predict whether a part design is subjected to fatigue failure. A generalized view of fatigue life diagrams is presented in Figure 7.

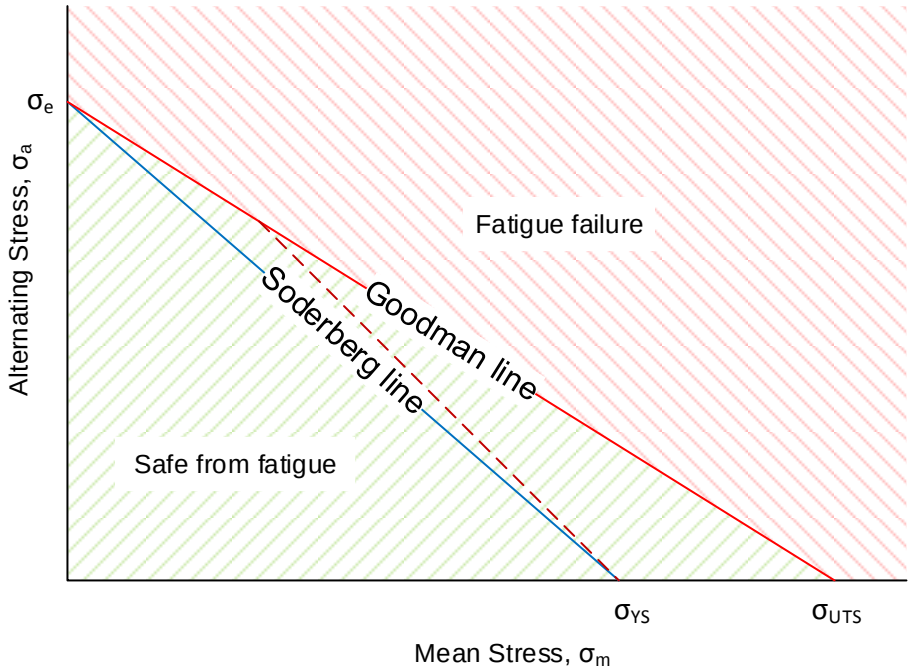

Figure 7: Goodman and Soderberg Diagrams – General Representation

Goodman and Soderberg lines can be described using the Equation (1) and Equation (2), respectively:

$$\sigma_a = \sigma_e \cdot \left(1 - \frac{\sigma_m}{\sigma_{UTS}}\right) \quad (1)$$

$$\sigma_a = \sigma_e \cdot \left(1 - \frac{\sigma_m}{\sigma_{YS}}\right) \quad (2)$$

The design can be considered as safe from fatigue failures (often called "infinite life region", highlighted in green in the figure above) if the point representing mean and alternating stresses in the component falls in the area enclosed between the X-Y axes and the Goodman or Soderberg lines (lower left region on the chart). On the other hand, a part with such stress combination that falls outside of the range enclosed by the axes and Goodman line is expected to have a fatigue failure at some point during service (or sometimes defined as "finite fatigue life", highlighted in red).

Clearly, the Soderberg line provides a more conservative estimate for the operating region by employing yield strength as the mean stress upper limit, where a part would be free from fatigue failures. Some deem the Soderberg line as overly conservative. Frequently, a modified Goodman diagram is used as a compromise between traditional Soderberg and Goodman lines. The modified Goodman line (shown as dashed line in Figure 7) starts at the point corresponding to the yield strength value on the mean stress axis and is directed at 45 degrees to the X-axis until intersection with the traditional Goodman line.

Also, the diagram shows that a relatively high mean stress in combination with what appears to be an insignificant alternating stress may lead to fatigue failure as well. This underlines the importance of having a significant safety factor in terms of steady state stresses for the components in the cases where alternating stresses are expected to be high. Control (Curtis) stage blades of steam turbines is one of the example for such components, where the cyclic loading is usually considered as quite significant due to partial steam admission.

In some cases, it is impossible to completely avoid high alternating stresses due to certain design or operational limitations. Thus, the only plausible solution is to minimize the high alternating stresses by introducing additional damping to the part. Shrouds in the blades, tie-wires in the blades and open-face impellers are good examples of such design modifications intended to minimize the alternating stresses.

Typical fracture surface due to fatigue would be flat and featureless. It may exhibit "beach marking" as example shown in Figure 8. Beach markings can provide a good indication of where the fatigue initiated and propagated.

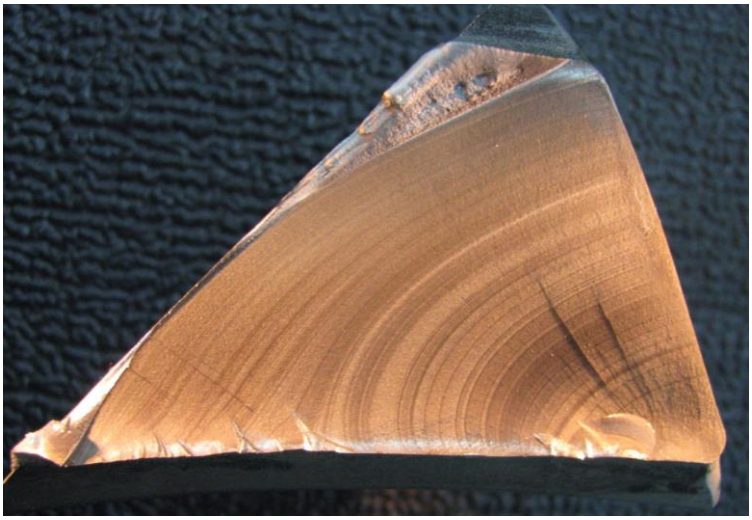

Figure 8: Fracture Surface of Blade Root Section Failed in Fatigue

In some cases, SEM evaluation may show striations which are also evidence of fatigue mode of failure. Striations on a fracture surface of a failed compressor blade are shown as an example in Figure 9.

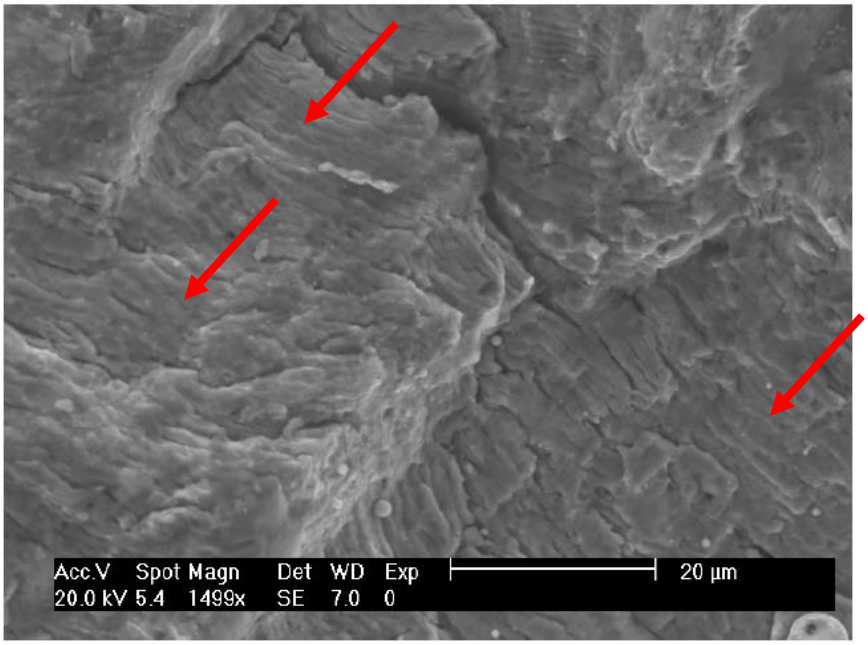

Figure 9: SEM Image of a Failed Compressor Blade Fracture Surface. Arrows point to some of the striations.

In addition to the design features, which may serve as stress concentrators (holes, fillets, notches), material conditions have an influence on the fatigue properties of a component. This includes the grain size, surface finish of the part, etc. An example of a steam turbine blade failure due to fatigue is shown in Figure 10. In this case, tie-wire hole in the last stage airfoil served as a stress concentrator (pointed by red arrow) and became the initiation location for the fatigue fracture. The crack propagated from the convex (suction) side towards trailing edge and concave (pressure) side of the airfoil, parallel to the direction indicated by the blue arrow.

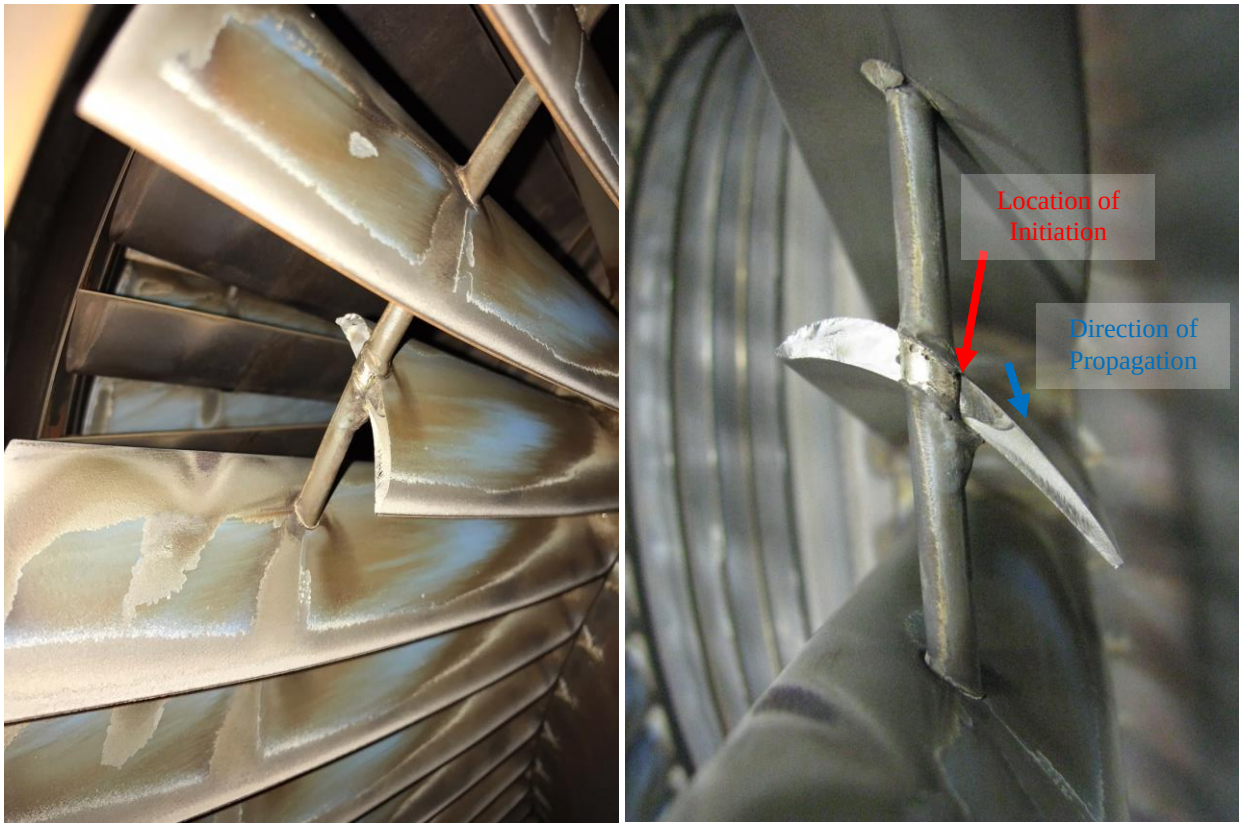

Figure 10: Fatigue Failure of Steam Turbine Blade

Corrosion Related Failures

The effect of corrosion can manifest itself into different types of damages. Corrosion in combination with erosion can reduce the effective cross section of a stressed component which may lead to failure due to overload. Localized corrosion can create a stress concentration that can lead to initiation of a fatigue failure. Similarly, corrosion-fatigue is a mechanism where the crack initiates and/or propagates due to the combined effect of cyclic/fluctuating stresses and a corrosive environment. The fatigue strength of a material in a corrosive environment goes down significantly compared to the fatigue strength under normal (non-corrosive) conditions. Figure 11 illustrates the difference between the fatigue strength of the same material in a normal and corrosive environment.

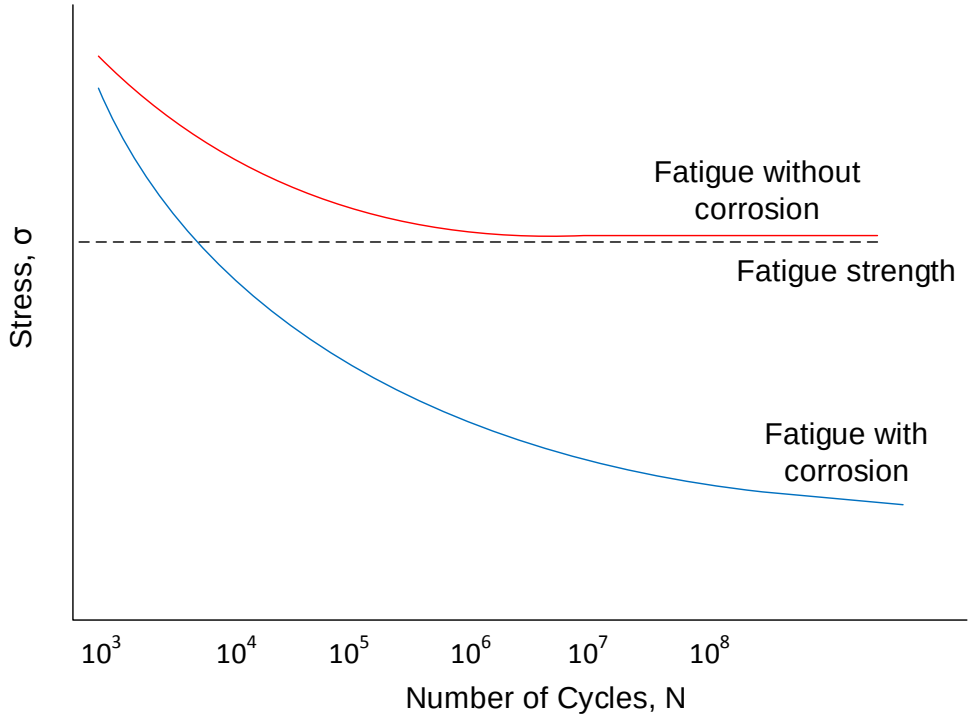

Figure 11: Fatigue Strength in Normal and Corrosive Environments

Stress Corrosion Cracking

Stress Corrosion Cracking (SCC) is another common mode of failure seen in steam turbines as indicated by Suss (1979) and Speidel et al (1991). The following three factors are required to be present for this type of failure to occur:

- Relatively high stress
- Material susceptible to corrosion
- Corrosive agents in the process gas

The level of stress required for stress corrosion cracking to occur under certain conditions varies depending on the severity of the environment and resistance of the material to SCC. Therefore, no universal guidance can be provided, but in the SCC cases known to the authors, the stresses in the cracked areas were as low as 40 percent of the yield strength of the material.

Stress corrosion cracking can occur in intergranular or transgranular fashion. Optical metallography through the crack would help to determine if the crack is transgranular or intergranular. Figure 12 shows examples of transgranular and intergranular cracks. In the figure on left, cracks are going through the interior of the grains in the micrograph, which is called transgranular cracking. In the figure on right, cracks are going along the grain boundaries in the micrograph, which is defined as intergranular cracking

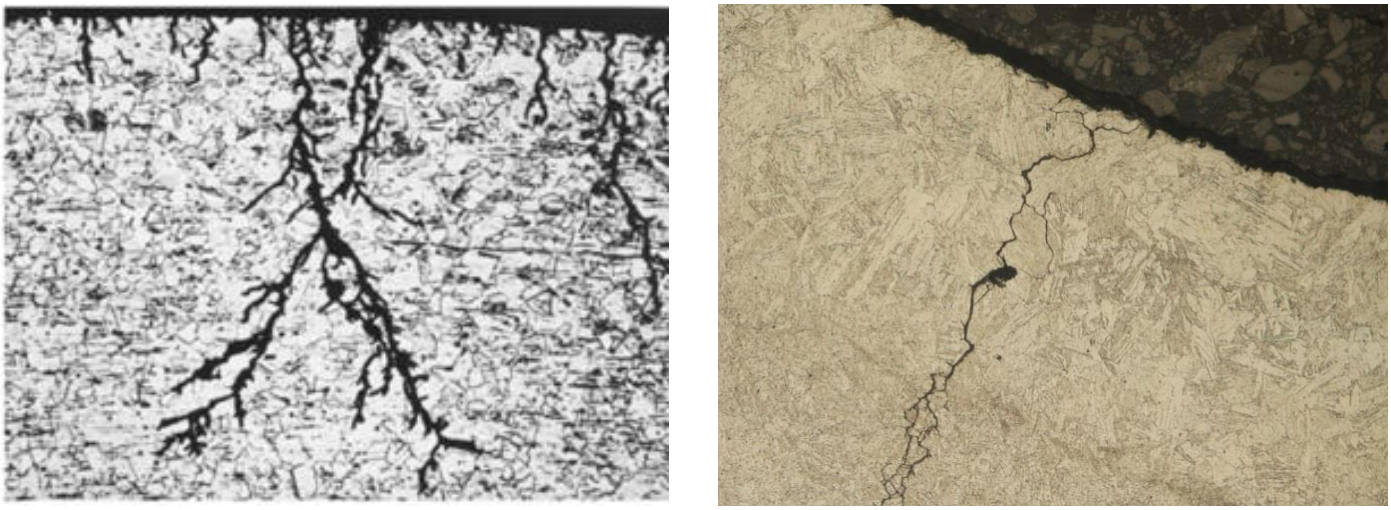

Figure 12: Transgranular (left, Balan (2018)) and Intergranular (right, failed impeller studied by the authors) Stress Corrosion Cracking

A surface with intergranular fracture would show different facets of grains as shown in Figure 13, which is an SEM fractograph of a cracked rotor. Facets of different grains can be seen. The failure had occurred along these facets of the grains.

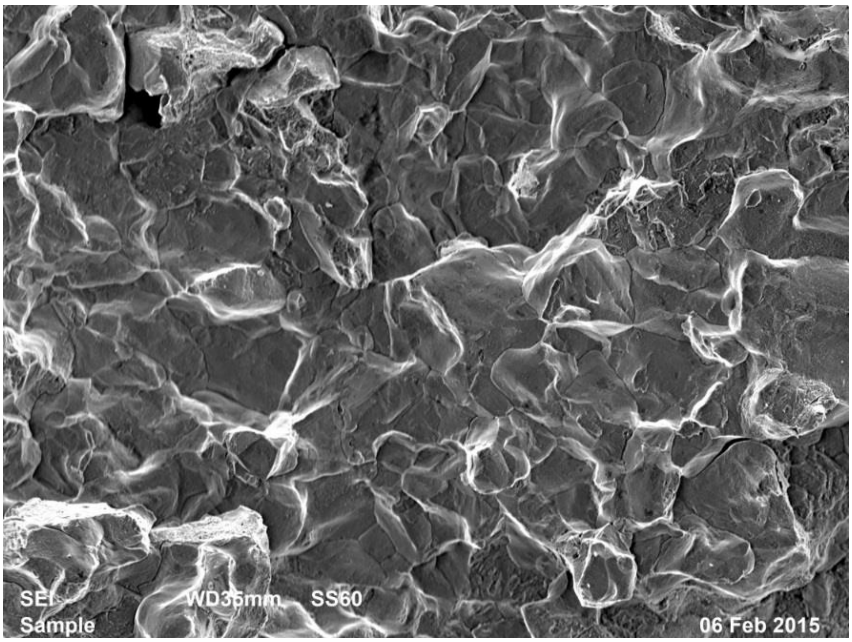

Figure 13: Intergranular Cracking in Steam Turbine Rotor (Gowreesan and Grebinnyk (2017))

An additional confirmation of corrosion-related nature of a failure can be obtained by examining the fracture surface using Energy-Dispersive Spectroscopy (EDS). Presence of oxygen, chlorine or sulfur on the fracture surface is an indication of the part being subjected to corrosive environment during service. Figure 14 shows results of EDS performed on the fracture surface of a steam turbine shroud (base material 17-4PH). The fracture surface had all the evidence of SCC and EDS confirmed the presence of corrosion products. Excessive amount of oxygen (20%) in combination with chlorine indicates highly corrosive environment and unsatisfactory water treatment at the steam turbine's facility. Abnormally high copper content (15%) was explained by the end-user as being carried over with steam from the turbine condenser piping.

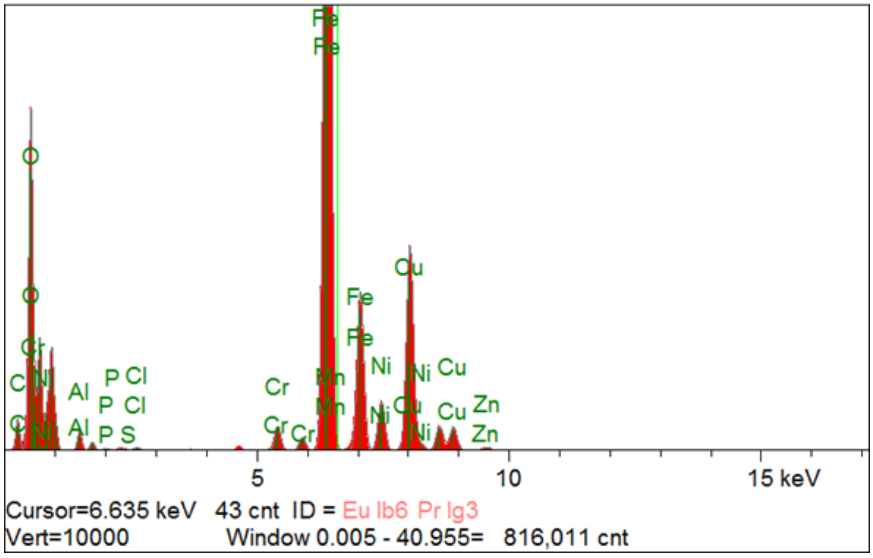

Element		Intensity (c/s)	Concentration	Units
C		7,054.0	7.530	wt.%
O		69,463.8	20.775	wt.%
Al		4,754.4	0.955	wt.%
Si		2,154.6	0.313	wt.%
P		667.6	0.080	wt.%
S		761.4	0.073	wt.%
Cl		1,012.6	0.089	wt.%
Cr		8,385.5	0.652	wt.%
Mn		3,693.4	0.368	wt.%
Fe		441,386.6	48.538	wt.%
Ni		18,849.8	3.083	wt.%
Cu		80,674.0	15.417	wt.%
Zn		9,768.5	2.127	wt.%
			100.000	wt.%

Figure 14: EDS Analysis of the Deposits on the Fracture Surface of a Steam Turbine Shroud

Discovery of an intergranular failure does not automatically mean that the mode of failure is stress corrosion cracking. Other failure mechanisms such as embrittlement and creep may also lead to intergranular cracking.

Embrittlement Related Failures

Embrittlement leads to weakening grain boundary as some atoms such as phosphorus, hydrogen or even cadmium, migrate to the grain boundaries. As a result, failure can occur in an intergranular fashion. Measurements of impact toughness or certain metallographic analysis are needed to confirm that the failure is related to embrittlement. Impact testing would show reduced value if the material is embrittled. Metallographic testing would look for the presence of embrittling elements at the grain boundaries. Typically, the mechanisms leading to embrittlement are related to exposure of the material to high temperature, below the tempering temperature of material, for extended periods of time.

Creep

This type of failure/deformation occurs when a component is under stress at elevated temperature for sustained period of time. In other words, creep can be defined as "thermally assisted time-depended deformation", as stated by Viswanathan (1989). Different alloys have different threshold temperatures for creep damage. Progression of creep is defined by three distinct phases: primary, secondary and tertiary. An idealized creep curve is shown in Figure 15. Primary creep is characterized by strain hardening. A few competing effects such as strain hardening, softening and material damage take place during the secondary phase. Secondary phase has nearly constant creep rate and may last for years depending on the applied loads and temperatures. During tertiary creep phase, the rate of strain is accelerated and results in a sudden rupture or failure.

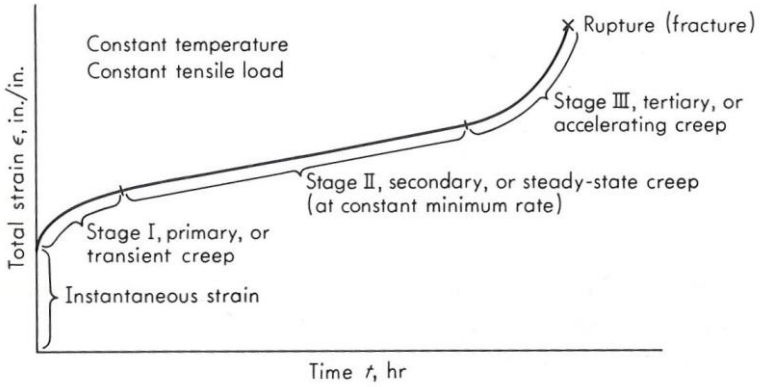

Figure 15: Idealized Creep Curve (Juvinall (1967))

Due to the actual creep processes spanning over multiple years, there was a need for the accelerated testing methodology, which would not require a significant amounts of time (hours or days instead of years) and can be reliably extrapolated onto years of service period. Over the past century, a number of different techniques for the prediction of creep have been developed and used by

turbomachinery, pressure vessel and other related industries. In this article, only the Larson-Miller parameter is reviewed, as it is one of the most commonly used parameters and is relatively simpler compared to other ones. Larson-Miller parameter is presented in Equation (3).

$$LMP = T(\log t + C) \quad (3)$$

In this equation, T is service or testing temperature (in absolute units) and t is time to rupture in hours. C is a constant that is typically equal to 20, but optimum value for it varies between 10 and 40 depending on the type of material.

A creep-rupture (also called stress-rupture) test is performed at a slightly elevated temperature compared to the actual service conditions but with similar stress levels. The time to rupture is recorded and the results can be extrapolated onto the actual service temperatures using the Larson-Miller parameter to define the projected service time.

Appearance of creep-related failures in most of the cases is intergranular and can look quite similar to the fracture surface shown in Figure 4. Non-destructive methods for detection of creep are quite limited. Dimensional inspections can be used to determine the change in a part's dimensions due to strain accumulation if the accurate, original dimensions are known. In-situ metallography, via collecting replicas from a part surface to detect changes in microstructure, may also provide some insight into progression of the creep. However, localization of the creep damage in highly stressed areas, such as disc and blade roots, may worsen an accurate assessment of the part's conditions with non-destructive testing. Only destructive testing including looking at the micrographs of the affected area along with the creep-rupture testing of the material in representative conditions may provide a complete understanding of the extent of creep damage.

Additional Information

Additional information on the failure mechanisms described above can be found in the following references: ASM Handbooks (1992) and (1994), Brooks and Choudhury (1993), Wulpi (2013).

CASE STUDIES

The following case studies are presented to illustrate the most common failure modes in the turbomachinery and demonstrate relationships between the different engineering disciplines for evaluations of the failures.

Case Study 1: Ductile Failure of Locking Pin

An axial-flow hot gas expander rotor failed its 3rd stage (R-3) locking blade. General view of the rotor in as found condition is shown in Figure 16.

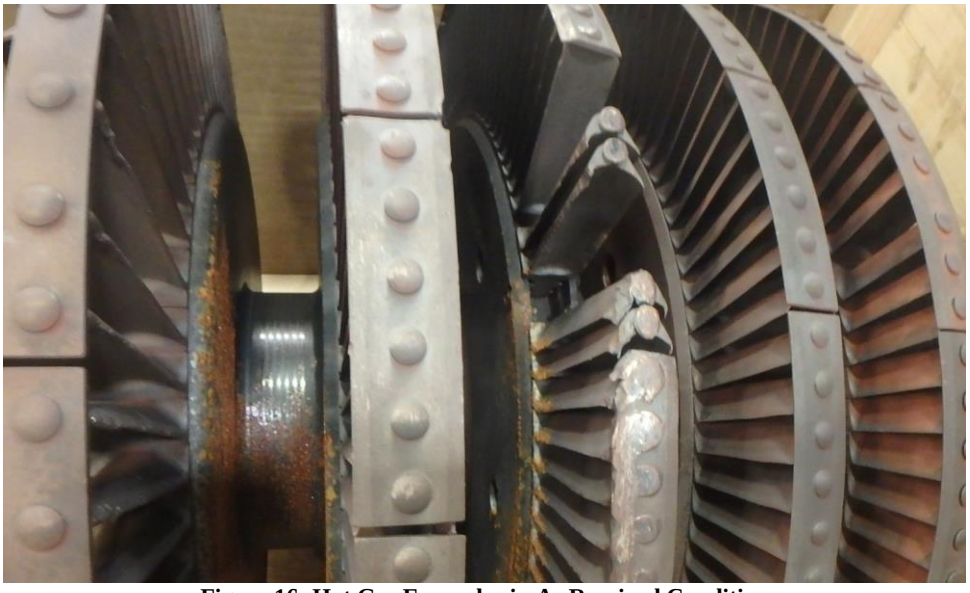

Figure 16: Hot Gas Expander in As Received Condition

The subject stage had tangentially loaded double-hook T-root blades and employed a double pin locking mechanism. Upon detailed visual inspection, it was found that the locking pin hole and the material above it had deformed quite significantly into an oblong shape, as shown in Figure 17.

Figure 17: R-3 Locking Pin Hole Material Deformation

The initial findings pointed towards ductile failure of the locking pin, therefore, additional steps were taken to determine the underlying reasons for such failure. Metallurgical evaluation of the remaining portions of the locking pin as well as steady state structural FEA were performed. Only three pieces of the two locking pins were found in place. Figure 18 illustrates the findings.

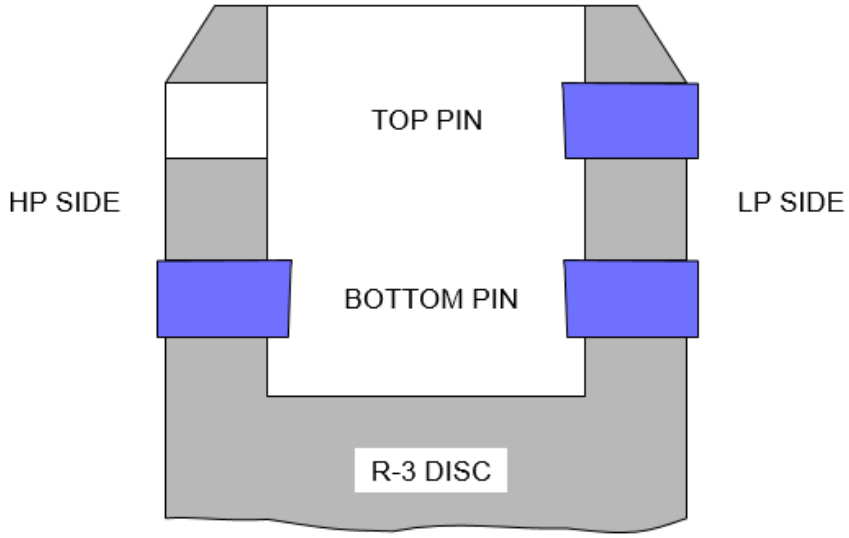

Figure 18: Sketch Showing the Locking Pin Pieces Found in the R-3 Disc

During examination of the fracture surface under SEM, significant deformation was found at the suspected crack initiation locations for both HP and LP sides of the bottom pin. Initiation locations are indicated by red arrows in Figure 19.

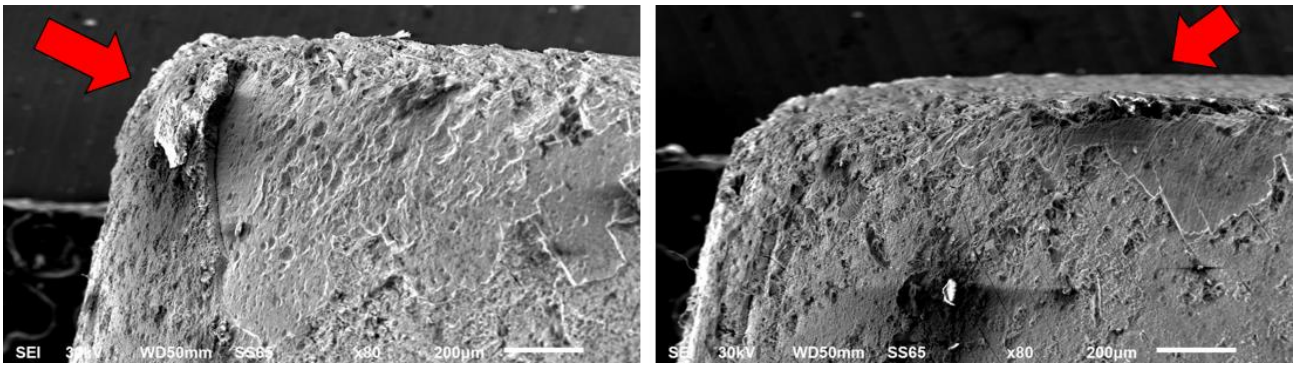

Figure 19: Suspected Fracture Initiation Location Found at the Bottom Pin Parts Under SEM

Additionally, the fracture surface did not display any mechanical defects, pitting or other evidences, which would be typical for fatigue or stress corrosion cracking. Almost the entire fracture surface of the parts showed what appeared to be a classic example of ductile failure with multiple dimples, as presented in Figure 20.

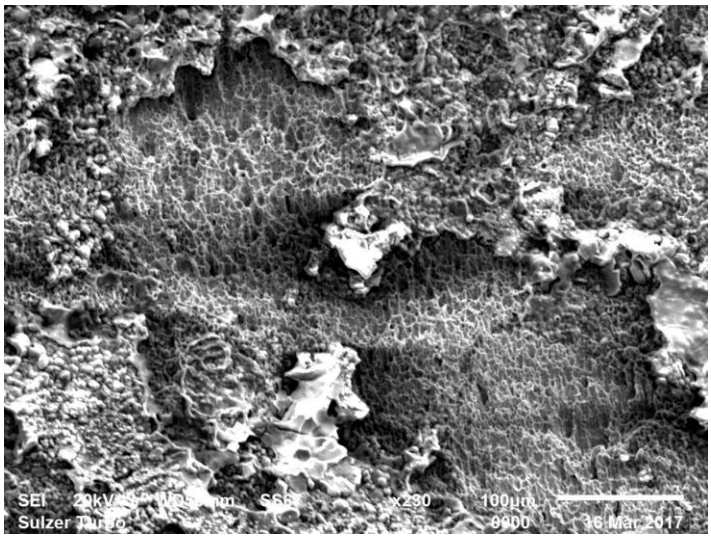

Figure 20. Top Pin Fracture Surface Showing Signs of Ductile Failure

Positive Material Identification (PMI) performed on all pieces of both pins confirmed that the material is H13 (tool steel). It was impossible to perform complete mechanical properties test due to the small size of the pieces. Hardness readings were collected using the polished and mounted samples of the pin. Measured hardness values ranged from 26 HRC to 30 HRC, and based on these findings, the yield strength of the pin was concluded to be approximately 110 ksi. A temperature of 800 °F was inferred for the 3rd stage blades based on the known inlet and outlet conditions for the hot gas expander. Therefore, the material's yield strength is expected to reduce to approximately 95 ksi during service. This results in shear strength equal to 54 ksi during operating. As a rule of thumb, the shear strength can be estimated as approximately 57% of the material yield strength.

A structural FEA was performed to determine stresses in the locking pins at operating speed. Thermally-induced loads were not taken into account to simplify the FEA problem setup. In this case, the thermal expansion coefficient for the pin, disc and blade materials are quite similar and the assembly would not experience additional temperature-related loads due to this. Due to thermal expansion coefficients of the pin, disc and blade material being quite similar and to simplify the FEA problem setup thermally-induced loads and effects, other than reduction in strength properties, were disregarded. The locking blade was recreated using the geometry of the regular blades from the same row since the actual locking blade was destroyed during the event. The locking blade 3D model used for the structural FEA is shown in Figure 21.

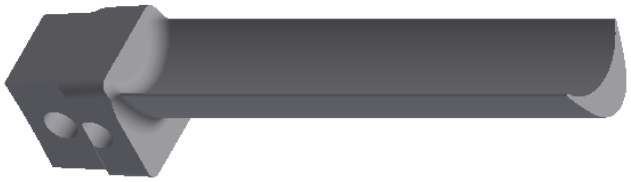

Figure 21: 3D CAD Model of the R-3 Locking Blade

Stresses were calculated at 100 percent and 115 percent of MCOS. These operating speeds correspond to normal operation and overspeed trip events, respectively. Equivalent (von Mises) stress at these conditions for the blade and pins is shown in Figure 22. To improve clarity, Figure 23 shows stresses in the pins at the same operating conditions.

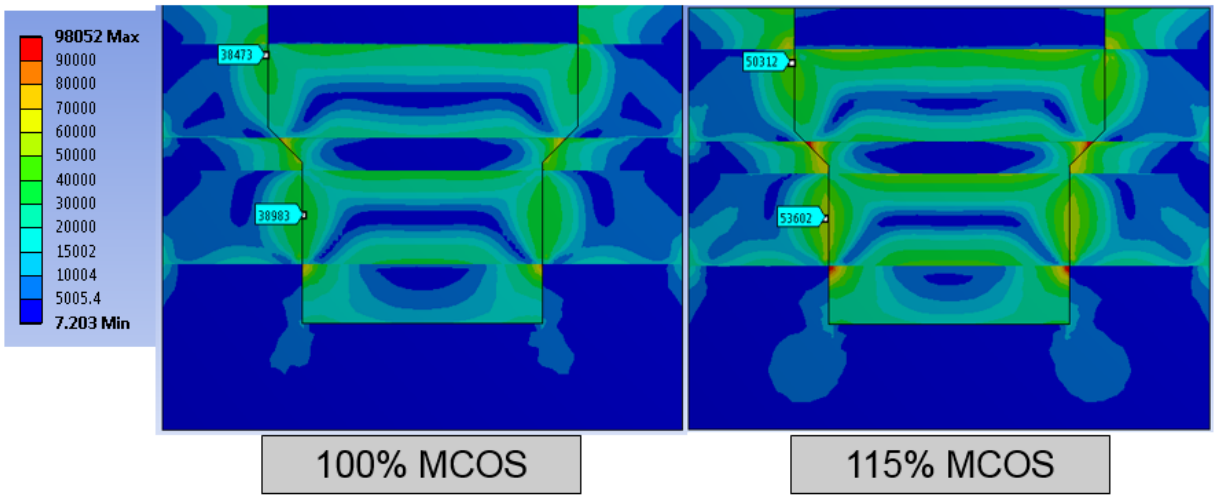

Figure 22: Equivalent Stress (psi) in the R-3 Locking Blade and Pins

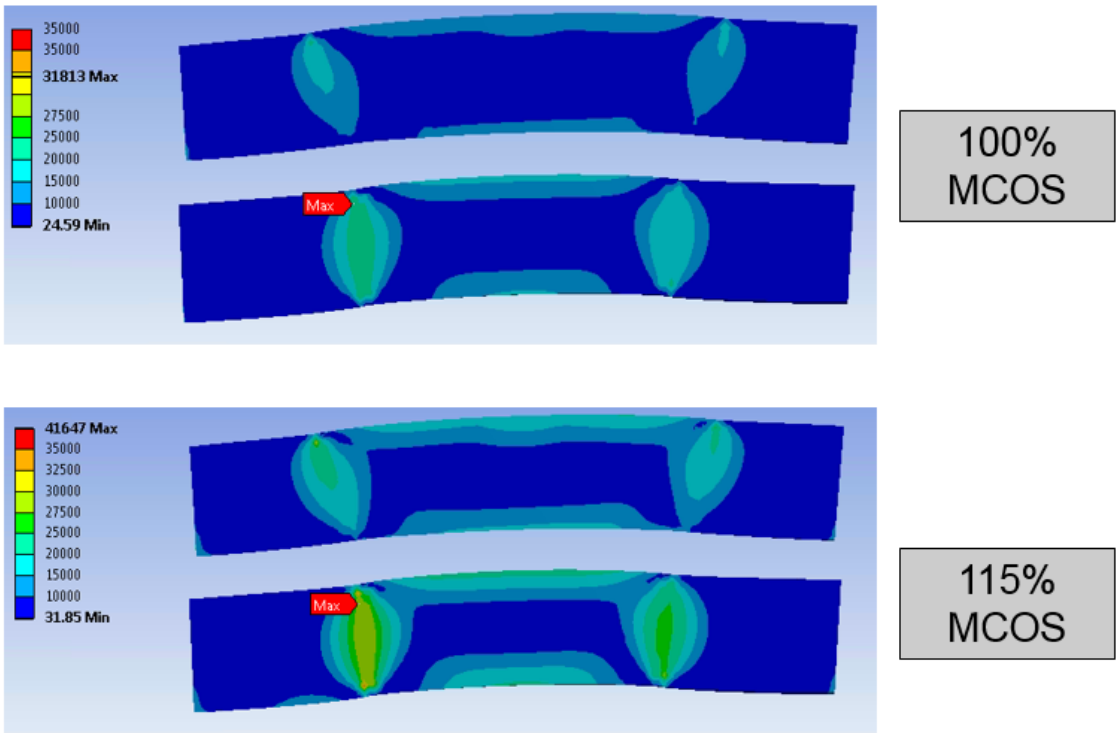

Figure 23: Equivalent Stress (psi) in the R-3 Locking Pins (Deformations Exaggerated)

By means of FEA the safety factor for the pins is equal to 1.3 at 115 percent of MCOS. In general, for the authors, it appeared to be marginally sufficient. However, based on conversations with the plant personnel it was found that this unit may have experienced some temperature excursions and possible overspeeding beyond 115 percent of MCOS during its service. Therefore, in order to improve the design, the following modifications were recommended. Firstly, upgrade the pin material to 422SS with hardness from 42 HRC to 48 HRC. This will provide an increase in yield strength to approximately 130 ksi during service, and, correspondingly, increase the shear strength of the material. The yield strength in shear can be estimated as approximately 57% of material's yield strength. Secondly, it was proposed to further increase the safety factor by employing a locking block design in lieu of the locking blade. Reduction of the mass carried by the locking pins will positively affect its safety factor and provide an additional assurance that the repetitive failures would be avoided.

Modifications were implemented to the expander design, but no further service history has been reported for the subject rotor since it has become the spare rotor.

Case Study 2 – Fatigue Failure of a Centrifugal Impeller

A centrifugal blower supplying process air at a plant has been removed from service for repairs after it tripped due to excessive vibration. The blower is a single stage, overhung, open-face impeller driven by a steam turbine, operating in a wide range of speeds (4,722 RPM – 7,083 RPM). Upon inspection, it was found that a piece from the backplate of the impeller was liberated causing excessive unbalance and high vibrations. The extent of the damage is shown in Figure 24. This was not an isolated incident as three other similar units reportedly failed in similar ways in the past. A failure analysis was performed to determine the inherent design flaw for the blower.

Figure 24: Backplate of the Impeller with Liberated Material Piece

The material of the impeller was identified as 17-4 PH stainless steel with a measured hardness of 28-35 HRC, which suggests that an approximate yield strength of the base material is 105 ksi. The analysis started with a metallurgical study of the fracture surface which identified high cycle fatigue (HCF) as the failure mechanism. In-situ replicas of the fracture surface were not clear enough to detetrmine the location of crack initiation. Destructive metallurgical testing could not be performed because the plant wanted to repair the existing impeller. A mechanical structural analysis followed after sufficient data was gathered from the plant, namely service history and conditions at the time of the failure. The steady state finite element analysis showed that the operating stresses were well within the elastic range of the material with a safety factor of over 2.0 at the equipment overspeed trip speed of 110% MCOS (Figure 25). The findings from the FEA agreed with the study of the fracture surface and dismissed any possibility of static overload as the cause of the failure.

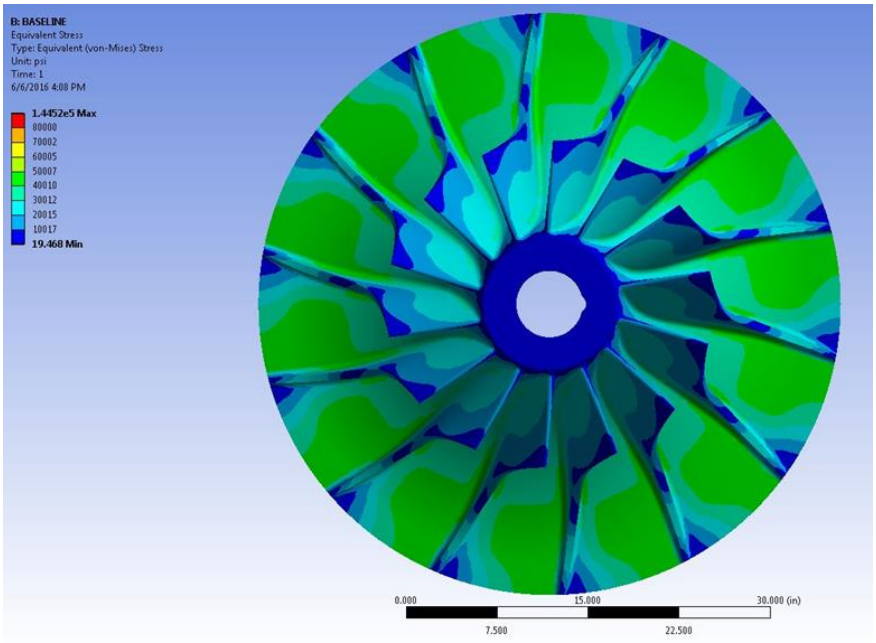

Figure 25: Equivalent Stresses (psi) at 110% MCOS

Since the metallurgical study results indicated that HCF is responsible for the failure, the next step in the engineering analysis was to determine any external sources of cyclic loading that could lead to excessive alternating stresses in the backplate. Most common or direct sources of cyclic loading in impellers are vane passing frequencies (VPF) from upstream and/or downstream stationary vanes (inlet guide vanes or diffusers). If these frequencies are close to a natural frequency of the impeller at a certain operating speed, then a state of resonance is imminent. VPFs can be calculated using the Equation (4),

$$VPF = \frac{Number\ of\ stationary\ vanes\ \times RPM}{60} \quad (4)$$

A modal analysis was performed to study the possibility of resonance being the cause of the failure. The impeller was impact (ring) tested to identify its natural frequencies and was compared to the predicted "free-free" natural frequencies from the FEA. Impact testing uses a calibrated accelerometer attached to the backplate and a hammer to impact individual points around the backplate. The result of the impact test are natural frequencies of the wheel and deflections (mode shapes) corresponding to them. The impact test setup is shown in Figure 26.

Figure 26: Impeller Impact Test Setup

Good correlation between the measured and numerically predicted frequencies proved the accuracy of the analytical 3D FEA

model. Vane passing frequencies were calculated and a pre-stressed modal FEA determined the natural frequencies in the operating speed range. Campbell and interference (also known as SAFE) diagrams for the stage showed two natural frequencies interfered with the 1xVPF from the downstream vaned diffuser in the speed range of 5,900-6,000 rpm (Figure 27 and Figure 28). Based on the impact test data and modal FEA, the mode shapes of both interfering natural frequencies were backplate-related and closely resembled the geometry of the liberated piece. After reviewing the operating data, the unit was held for prolonged periods inside the range of 5,900–6,000 rpm, a low speed regime at which the plant operated at reduced flow rates without venting air.

Detailed theoritical background of Cambell and SAFE diagrams is given by Singh (2013). Singh provides the fundamental framework to predict and advoid resonance in turbomachinery components (bladed turbine disks and impellers), as well as highlights historical developments in this area.

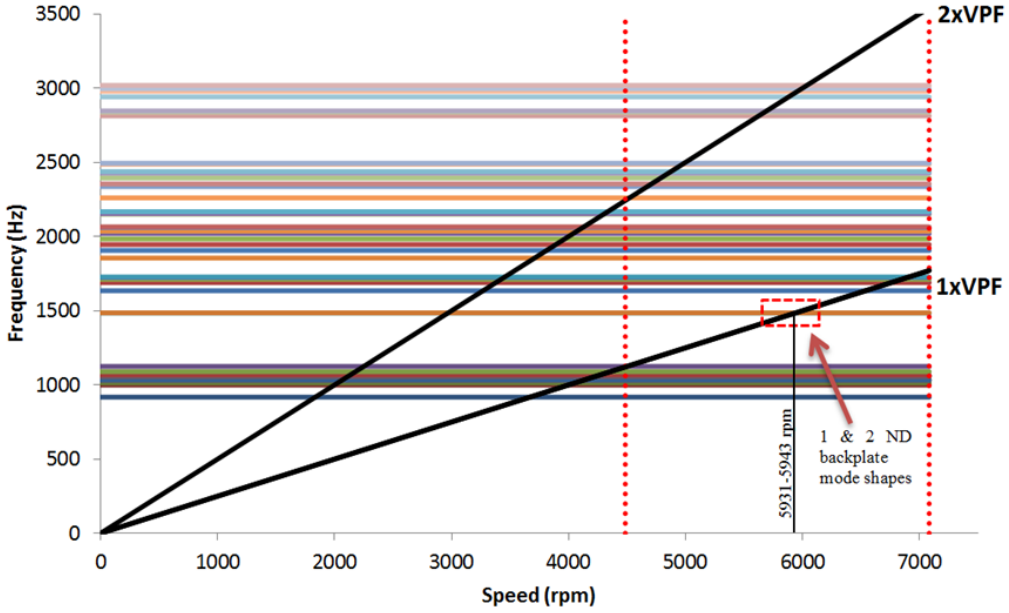

Figure 27: Campbell Diagram for the Impeller (Baseline Design)

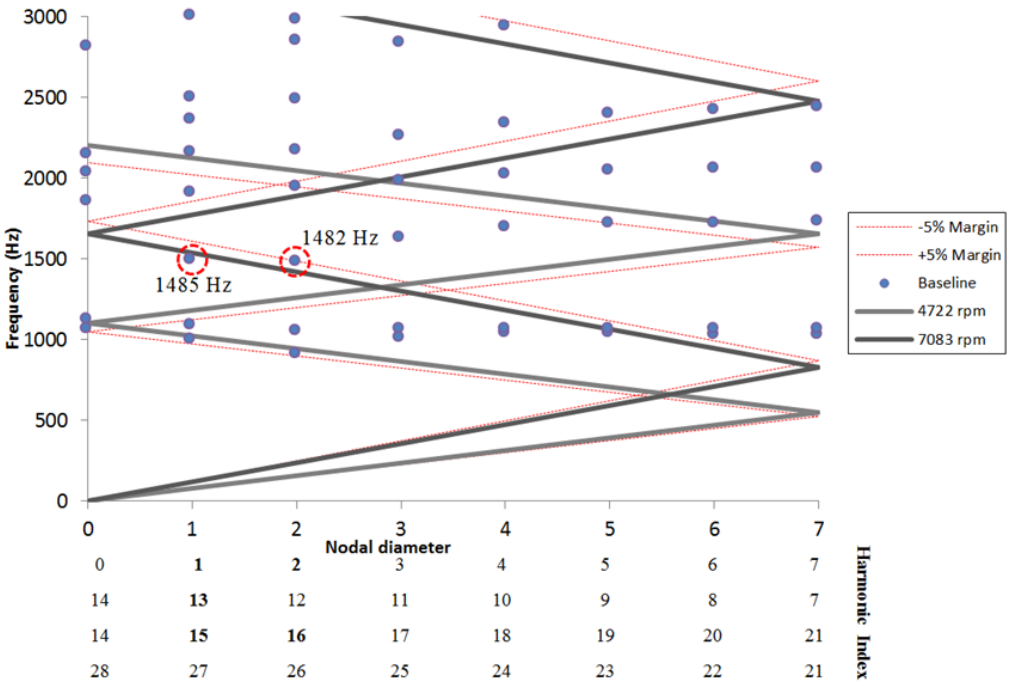

Figure 28: Interference (SAFE) Diagram for the Impeller (Baseline Design)

Major design changes must be made to the structure to completely avoid resonance issues in the impeller. This could include changing the impeller's material and construction or modifying the number of vanes in the stationary components, all of which are not

cost/time efficient for the constraints given. Instead, the solution was to machine cut-outs to the backplate of the existing impeller, typically referred as “scallops” (Figure 29). This allowed to change the impeller’s natural frequencies and to successfully move them out of the interference range. Campbell and SAFE diagrams for the redesigned impeller are shown in Figure 30 and Figure 31 respectively. Additionally, two safe operating speed ranges were defined within which the blower could operate at lower and higher speeds depending on the plant’s air demand. It was advised to the end-user to avoid operating outside of the speed ranges defined as safe.

Impact testing performed on the final design confirmed that the natural frequencies no longer interfere with the vane passing frequency within the defined operating speed ranges. The redesigned impeller has been put in service and no further issues have been reported since then.

Figure 29: Impeller Geometry after Modification with “Scallops”

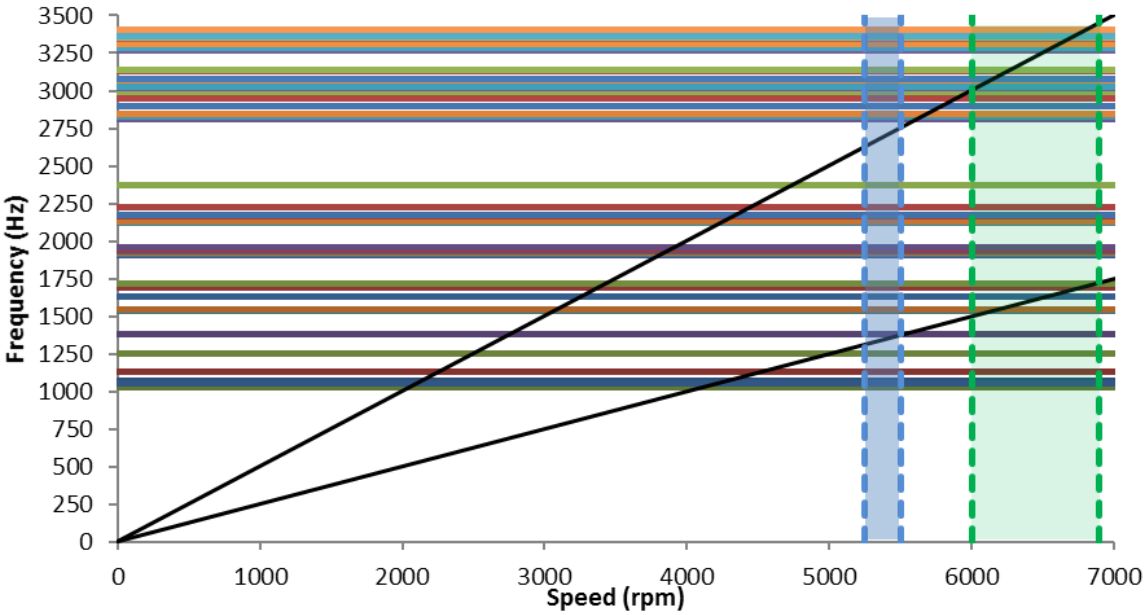

Figure 30: Campbell Diagram for the Impeller (Modified Design)

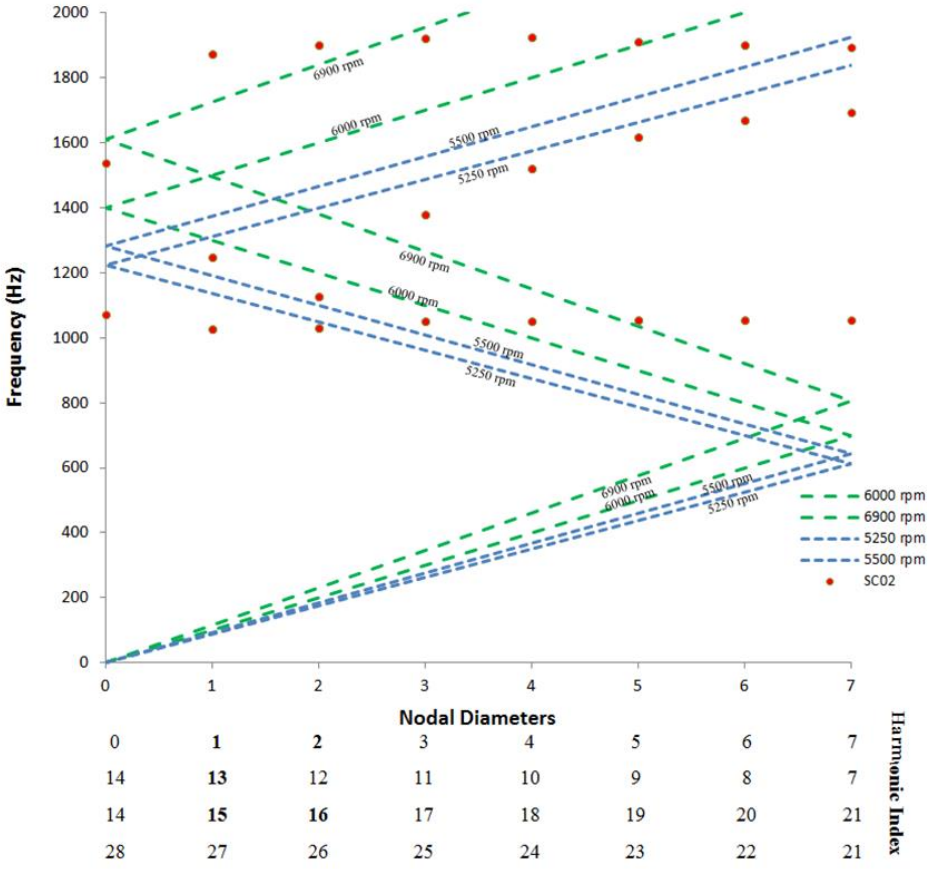

Figure 31: Interference (SAFE) Diagram for the Impeller (Modified Design)

Case Study 3 – Corrosion Fatigue Failure of a Blade

A crack developed in a blade (11th stage) of a steam turbine. The crack was located near the bottom of the trailing edge side of the blade as outlined in Figure 32.

Figure 32: Stage 11 Blade with Crack to the Trailing Edge

The cracked blade was mechanically opened to evaluate the fracture surface. Visual and stereo microscope evaluation showed that the fracture surfaces on both sides were flat until the crack changed direction. Faint evidence of beach markings, which is a telltale sign of fatigue, can be seen in some areas of the fracture surfaces as shown in Figure 33. The red arrows point to the primary fracture plane. The green arrows point to the secondary cracks on the convex side of the vane as shown by the inset at the lower right corner of the Figure. The blue arrows point to a secondary fracture plane on the concave side of the vane and these two cracks correspond to the magnetic particle indications (cracks) shown in the inset at the top left corner of the Figure.

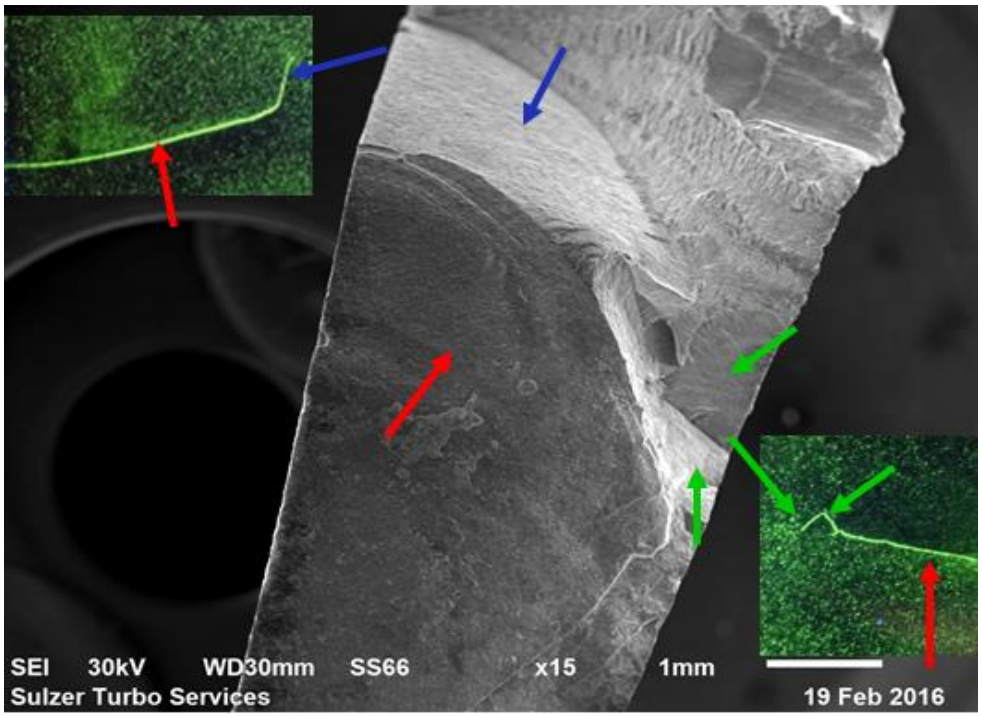

Figure 33: SEM image of the fracture with different fracture plane.

Figure 34 shows an SEM image of the fracture surface closer to the trailing edge of the blade. The blue arrows point to the pattern indicating the initial crack propagation region. The general surface area appears to be flat which itself is typical if crack propagation is due to fatigue. The fatigue propagation pattern appeared to indicate that the crack initiated at the corrosion damage pointed by the red arrow. This is deduced from the tiny light colored lines that seem to initiate from the area pointed by the red arrow. Corrosion pitting can be seen in the adjacent areas. The green arrow points to additional corrosion damage at the leading edge. The region of an impact damage in the fracture plane is indicated by the yellow arrow.

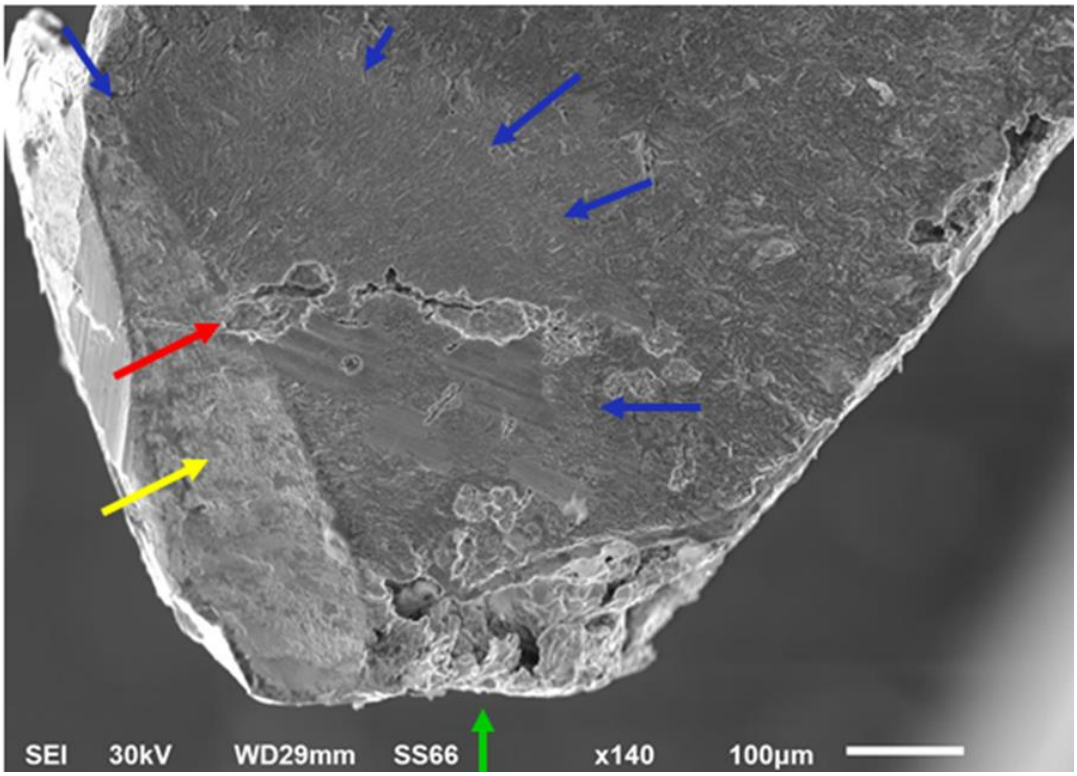

Figure 34: SEM Image of Fracture Surface at the Trailing Edge of the Blade

An energy dispersive spectroscopy (EDS) analysis showed an oxide layer on the fracture surface, with less deposits present away

from the trailing edge. This means that the fracture surface closer to the trailing edge was exposed for a longer duration than the fracture surface towards the leading edge. It is most likely that this crack initiated due to local crevice corrosion cracking and its orientation was determined by location of the crevices. Further evidence of independent crevice corrosion can be found on the blade surface as shown in Figure 35, where green arrows point towards the corrosion pits on the surface.

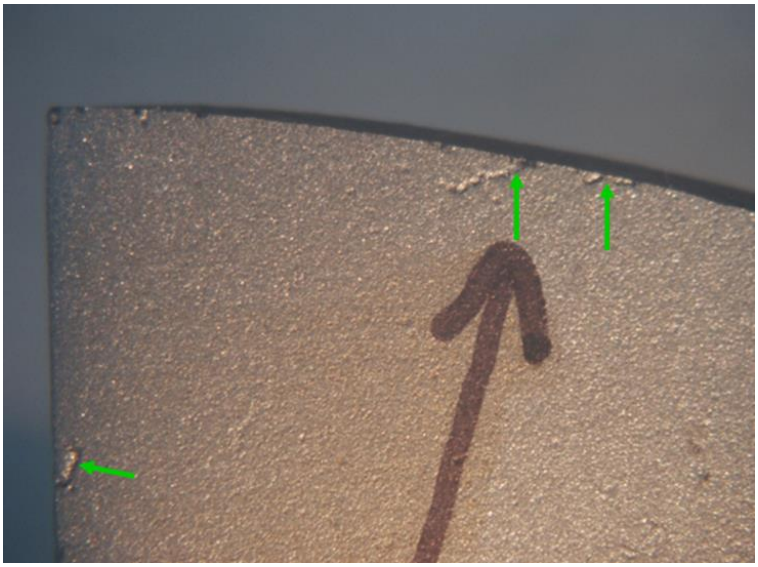

Figure 35: Side View of the Cracked Blade with Corrosion Pits

The material of the blade is identified to be 410SS from the chemical analysis results. Nothing abnormal was found when the room temperature mechanical properties were tested, all results were within the expected ranges for the material and application. Metallography confirmed that microstructure of the material is adequate and represents properly tempered martensite. Therefore, there is no reason to suspect that the crack was caused by reduced mechanical properties due to improper heat treatment of the material.

Based on all these observations, it is believed that crack initiated due to localized corrosion. This localized corrosion combined with cyclic loading led to the crack propagating in fatigue mode. At the time of inspection, only one blade with developed cracking was found though evidence of corrosion could be seen in most of the blades on row 11. The following measures were suggested to minimize the incidence of localized corrosion:

- Improving water treatment to obtain cleaner steam (reducing corrosive elements, such as chlorine)
- Application of sacrificial coating with cathodic protection to the blades
- Surface treatment of the blades to create compressive stress in them. Examples of such surface treatment are shot peening, laser shock peening, low plasticity burnishing and others.

Redesigning the blades to avoid fatigue seemed to be a premature solution in this case. As it was explained earlier, presence of corrosive agents deteriorates the material fatigue strength properties. Therefore, it's possible for fatigue to appear even in components whose design is considered appropriate for the normal environment. There is no solid guarantee that the pitting and subsequent fatigue damage cannot reappear in a different area unless the corrosion component is eliminated.

CONCLUSIONS

Failure analysis of mechanical components is an extensive subject. Although there is a finite number of failure modes, there could be a number of different ways to arrive to the same conclusion for engineers performing an investigation. Thus, the authors found it challenging to provide step-by-step instructions on how to resolve each specific case. This Tutorial is an attempt to summarize the most common failure modes in turbomachinery components and critical pieces of information required to make an informed conclusion about the reasons for failure. At the end of the day, the scope and extent of each specific investigation are going to be highly dependent on the impact of the failure and budget allocated. While some failure investigations may turn into full-scale research projects, others can be concluded after very basic material testing and engineering calculations.

Similar considerations apply to decisions about the steps to mitigate a failure. Careful considerations of all aspects must be made before attempting any design or material changes to ensure that the cure applied is not worse than the disease itself.

NOMENCLATURE

T	= Temperature	(°F)
t	= Time	(hr)
σ	= Stress	(psi)
σ_a	= Alternating stress	(psi)
σ_e	= Fatigue strength	(psi)
σ_m	= Mean stress	(psi)
σ_{UTS}	= Ultimate Tensile Strength	(psi)
σ_{YS}	= Yield Strength	(psi)

CFD = Computational Fluid Dynamics
EDS = Energy Dispersive Spectroscopy
FEA = Finite-Element Analysis
HCF = High-Cycle Fatigue
HP = High-Pressure
HRC = Hardness, Rockwell "C" Scale
MCOS = Maximum Continuous Operating Speed
NDE = Non-Destructive Examination
LCF = Low-Cycle Fatigue
LP = Low-Pressure
PMI = Positive Material Identification
R-1 = Turbine Row 1 Blades
RPM = Revolutions Per Minute
SEM = Scanning Electron Microscope
SCC = Stress Corrosion Cracking
TEM = Transmission Electron Microscope
VPF = Vane Passing Frequency

FIGURES

REFERENCES

ASM Handbook, 1992, *"Failure Analysis and Prevention"*, Vol. 11, ASM International, USA

ASM, 1994, *"Handbook of Case Histories in Failure Analysis Vol. 1 and Vol. 2"*, ASM International, USA

Balan, K. P., 2018, *"Metallurgical Failure Analysis: Techniques and Case Studies"*, Elsevier, pp 9-10.

Boyer, H.E., 1986, *"Atlas of Fatigue Curves"*, ASM International, USA

Brooks., C. R., Choudhury., A., 1993, *"Metallurgical Failure Analysis"*, McGraw-Hill, USA

Gowreesan, V., Grebinnyk., K., 2017, "Stress Corrosion Cracking In Steam Turbine – Two Case Studies", *Proceedings of the Turbomachinery Technical Conference and Exposition, ASME TURBO EXPO 2017*, Charlotte, NC, USA.

Jonas, O., 2008, "Steam Turbine Corrosion and Deposits Problems and Solutions", *Proceedings of the Thirty-Seventh Turbo Machinery Symposium*, College Station, TX, USA, pp 211- 228.

Juvinall R.C., 1967, *"Engineering Considerations of Stress, Strain and Strength"*, McGraw-Hill, USA

Lynch., S.P., Moutsos., S., December 2006, "A Brief History of Fractography", *Journal of Failure Analysis and Prevention*, Vol. 6, Issue 6, pp 54-69.

Horseman., G., 2015, "Latest Developments in Steam Turbines", *9th International Charles Parsons Turbine and Generator Conference*, Loughborough, UK.

Speidel. M.O, Denk., J., Scarlin., B., 1991, "Stress Corrosion Cracking and Corrosion Fatigue of Steam-turbine Rotor and Blade Materials", *Commission of the European Communities Report EUR 13186 EN*, pp. 23.

Suss, H., May 1979, "Evaluating Components Failures: The Cure can be Worse than the Illness", *Metal Progress, Vol 109 (No. 5)*, pp 26-29.

Viswanathan., R., 1989, *"Damage Mechanisms and Life Assessment of High-Temperature Components"*, ASM International, Ohio, USA, pp 59-103.

Wulpi., D, 2013, *"Understanding How Components Fail"*, Third Edition, ASM International, USA

BIBLIOGRAPHY

McGarry, D., 2002, *Course 0335 "General Procedures for Failure Analysis"*, ASM International

Singh, M., 2013, "History of Evolution, Progress and Application of SAFE Diagram for Tuned and Mistuned Systems", *Proceedings of the Forty-Second Turbomachinery Symposium*, Houston, Texas

ACKNOWLEDGEMENTS

Authors would like to thank all members of the Sulzer family for supporting their engineering endeavors.